Original Article

MOLECULAR METABOLISM

Roux-en-Y gastric bypass surgery reprograms enterocyte triglyceride metabolism and postprandial secretion in rats

Sharon Kaufman [1,*], Myrtha Arnold [1], Abdiel Alvarado Diaz [2], Heike Neubauer [3], Susanne Wolfrum [4], Harald Köfeler [5], Wolfgang Langhans [1], Jean-Philippe Krieger [6]

ABSTRACT

Objective: Roux-en-Y gastric bypass (RYGB) surgery produces rapid and persistent reductions in plasma triglyceride (TG) levels associated with fewer cardiovascular events. The mechanisms of the reduction in systemic TG levels remain unclear. We hypothesized that RYGB reduces intestinal TG secretion via altered enterocyte lipid handling.

Methods: RYGB or Sham surgery was performed in diet-induced obese, insulin-resistant male Sprague—Dawley rats. First, we tested whether RYGB reduced test meal-induced TG levels in the intestinal lymph, a direct readout of enterocyte lipid secretion. Second, we examined whether RYGB modified TG enterocyte secretion at the single lipid level and in comparison to other lipid subclasses, applying mass spectrometry lipidomics to the intestinal lymph of RYGB and Sham rats (0—21 days after surgery). Third, we explored whether RYGB modulated the metabolic characteristics of primary enterocytes using transcriptional and functional assays relevant to TG absorption, reesterification, storage in lipid droplets, and oxidation.

Results: RYGB reduced overall postprandial TG concentrations compared to Sham surgery in plasma and intestinal lymph similarly. RYGB reduced lymphatic TG concentrations more than other lipid subclasses, and shifted the remaining TG pool towards long-chain, unsaturated species. In enterocytes of fasted RYGB rats, lipid uptake was transcriptionally (*Fatp4*, *Fabp2*, *Cd36)* and functionally reduced compared to Sham, whereas TG reesterification genes were upregulated.

Conclusion: Our results show that RYGB substantially reduces intestinal TG secretion and modifies enterocyte lipid absorption and handling in rats. These changes likely contribute to the improvements in the plasma TG profile observed after RYGB in humans.

Keywords RYGB; Intestinal lymph; Enterocyte metabolism; Dyslipidemia; Obesity

1. INTRODUCTION

Bariatric surgery is currently the most effective treatment for obesity and its related comorbidities [1]. Along with the rapid remission of insulin resistance, the beneficial effects of bariatric surgery, and specifically RYGB, on cardiovascular diseases (CVD) are astonishing. Epidemiological studies report a drastic reduction of cardiovascular deaths (59% lower in RYGB compared to matched controls) and lower incidence of cardiovascular events in obese adults [2,3].

Dyslipidemia is the foremost modifiable risk factor of atherosclerotic CVD [4]. Therefore, the rapid and long-lasting improvements in the blood lipid profile (TG and cholesterol) commonly seen after RYGB may mediate these positive effects on CVD health [5,6]. Indeed, patients with TG levels remaining high (>160 mg/dL) after RYGB did not show a lower CVD incidence compared to the matched obese controls, indicating a causal relation between the decrease in TG levels and the decrease in CVD deaths [2,5]. How RYGB decreases plasma TG levels, however, is unclear.

Weight loss and improved insulin sensitivity are obvious candidate mediators for the reduced TG levels after RYGB, but they cannot entirely account for the rapid reduction in plasma TG levels [7,8]. In humans and animal models, many of the beneficial effects of RYGB, such as the improvements in plasma lipids or changes in bile acid metabolism, occur prior to and largely independent of weight loss. Also, an equivalent weight loss induced by caloric restriction does not produce similar improvements [9—11]. The intestine may contribute to the RYGB-improvements in the TG profile, as it absorbs dietary lipids and secretes chylomicrons in a controlled manner [12]. In the intestinal lumen, emulsified dietary TG are broken down by lipases, and the resulting fatty acids and monoglycerides are absorbed by the enterocytes [12]. After re-esterification, TG are

[1]Physiology and Behavior Laboratory, ETH Zurich, Schwerzenbach, Switzerland [2]Excercise and Health Laboratory, ETH Zurich, Schwerzenbach, Switzerland [3]Department of Cardiometabolic Diseases Research, Boehringer Ingelheim Pharma GmbH and Co. KG, 88397 Biberach/Riss, Germany [4]Laboratory of Organic Chemistry, ETH Zurich, Zurich, Switzerland [5]Core Facility Mass Spectrometry Lipidomics Research Center Graz, Austria [6]Epidemiology, Biostatistics and Prevention Institute, UZH, Zurich, Switzerland

*Corresponding author. Physiology and Behavior Laboratory, Institute of Food, Nutrition and Health, Schorenstrasse 16, 8603 Schwerzenbach, Switzerland. E-mail: sharon@kaufman.ch (S. Kaufman).

Received January 22, 2019 • Revision received March 3, 2019 • Accepted March 7, 2019 • Available online 13 March 2019

https://doi.org/10.1016/j.molmet.2019.03.002

Abbreviations

APOB	apolipoprotein B
LPC	lysophosphatidyl-choline
AUC	area under the curve
ORO	oil red O
CVD	cardiovascular diseases
PC	phosphatidylcholine
DDA	data dependent acquisition
PI	phosphatidylinositol
DG	diglyceride
PLS-DA	partial least squares discriminant analysis
FAO	fatty acid oxidation
RYGB	Roux-en-Y gastric bypass
FAU	fatty acid uptake
SM	sphingomyelin
FC	fold change
TG	triglyceride
HFD	high fat diet
TM	test meal
LFD	low fat control diet
VIP	variables importance on projection

mainly packaged into chylomicrons to enter the lacteals in the intestinal villi [13]. However, some of the absorbed lipids are also stored in the enterocyte in cytosolic lipid droplets or oxidized [14]. After RYGB, the Roux limb shows hyperplasia and hypertrophy [15,16], and enterocyte functions are modulated. This has been documented for enterocyte carbohydrate absorption and metabolism [17], but it is reasonable to assume that enterocyte TG handling is also affected by RYGB.

We therefore investigated whether RYGB affects enterocyte TG release and/or enterocyte TG metabolism using a rat model of RYGB. First, we tested *in vivo* whether the reduced postprandial TG concentrations, well documented in the plasma of RYGB rats, are also evident in the intestinal lymph, which provides the most direct readout of intestinal lipid secretion. Second, using a lipidomics approach, we examined whether RYGB specifically changes the concentrations of individual TG species and of diglycerides (DG), lipids that are also abundantly present in the lymph and are strongly associated with insulin resistance and T2DM [18]. Finally, we tested in primary enterocytes whether RYGB affects enterocyte lipid handling pathways, including TG absorption, reesterification, storage in lipid droplets, and oxidation. The results reveal substantial RYGB-induced changes in enterocyte lipid handling and indicate that these changes likely contribute to the RYGB-induced improvement in plasma TG levels.

2. MATERIALS AND METHODS

2.1. Animals and housing

Male Sprague Dawley rats (Charles River, Sulzfeld, Germany) were individually housed (21 ± 1 °C, 55 ± 5% relative humidity) with a 12 h light/12 h dark cycle. Unless otherwise noted, all animals had continuous ad libitum access to water and high fat diet (HFD, 60 kJ% fat, SSNIFF HFD, D12492, Germany). Four littermates kept on a low fat control diet (LFD, 10 kJ% fat, SSNIFF LFD, D12450B, Germany) served as a metabolically healthy control group. All procedures were approved by the Zurich Cantonal Veterinary Office.

2.2. IP glucose tolerance test and postprandial plasma triglyceride measurements

One week prior to and two weeks after the bariatric surgery (see below), rats were food deprived for 13 h and injected intraperitoneally (IP) with a 30% glucose in water solution (1.5 g/kg BW). Tail vein blood samples were taken for glucose measurements (Accu-Check Aviva blood glucose monitor, Roche, Switzerland). The same procedure was employed to measure plasma TG (Cobas Mira analyzer, Roche; Kit from Diatools, Villmergen, Switzerland) in blood taken 4 and 16 h prior to and 30 min after completion of a HFD test meal (TM) of 2.5 g (regular HFD at a restricted dose), which the rats ate within 10 min.

2.3. Intestinal lymph duct cannulation

Catheters were prepared and implanted as described before with slight modifications [19]. Rats (600–730 g) were fasted overnight and gavaged with 1.5 mL olive oil 2 h prior to anesthesia to increase intestinal lymph flow. Shortly before surgery, animals were subcutaneously (SC) injected (1 mL/kg BW) with 5 mg/kg enrofloxacin (Baytril, Bayer Vital GmbH, Germany) and anaesthetized (2–3% isoflurane (IsoFlo®, Abbott, Switzerland) in oxygen (Conoxia, Pan Gas, Switzerland). A polypropylene mesh with the sampling port was implanted SC between the scapulae. The superior mesenteric lymph duct, parallel to the mesenteric artery, was incised longitudinally, and the end of the polyurethane tubing was inserted to stabilize the lymph duct vessel, then a thin polyurethane tubing was inserted through the side hole and secured with tissue adhesive. Five mg/kg Carprofen (Norocarp, UFAMED AG, Switzerland) was injected for 2 days after surgery. Catheters were flushed daily with NaCl and refilled with heparinized 50% glycerol. The rats were allowed to recover for 14 days until the next surgery.

2.4. Roux-en-Y gastric bypass surgery

Three days prior to surgery rats were adapted to eat a porridge mesh mixture of oat flakes in water (ratio 1:3). Twelve hours prior to surgery the rats were food deprived and randomly allocated to the RYGB and Sham group. Surgical anesthesia and medication were the same as described for the lymph duct cannulation, with two added days of analgesic treatment post-surgery. The RYGB and Sham procedures were performed as previously described [20]. Briefly, the small intestine was transected 20 cm distal to the pylorus. The proximal end of the small intestine with the connected remaining part of the stomach (the biliopancreatic limb) was anastomosed to the ileum approximately 25–30 cm from the cecum, thus forming the common channel. Transection of the stomach about 5 mm distal of the gastroesophageal junction generated the gastric pouch of 2–3% of the original stomach size. Finally, the distal end of the small intestine was connected to the gastric pouch, forming the alimentary limb. For the Sham surgery, a gastrostomy and a jejunostomy were performed. After surgery, the rats were kept in a recovery cage without bedding for one day, with half the floor area covered by a heating pad. For the first 6 h after surgery, 6 mL of warm 0.9% NaCl were injected SC. Approximately 12 h later, rats were given access to water and offered a few grams of the porridge mesh. A few hours later, they had ad libitum access to the porridge mesh with progressive access to their original HFD until post-operative day four.

2.5. Intestinal lymph sampling

Five, 10, and 21 days after RYGB or Sham surgery the rats were offered a 2.5 g HFD TM after 6 h food deprivation. The rats were trained to complete this TM within 10 min. Time point "0 min" was marked as soon as the rat started to eat and 60 μL of lymph was

sampled at time points 25–29 min and 43–47 min as described earlier [21]. The lymph of both time points was pooled. Samples were kept on ice for 45 min (max), centrifuged, and supernatants stored at −80 °C until further processing.

2.6. Mass spectrometry lipidomics analysis of intestinal lymph

Seven lipid categories were analyzed: TG ($n = 81$), DG ($n = 22$), Phosphatidylinositol (PI, $n = 12$), Phosphatidylethanolamines (PE, $n = 16$), Phosphatidylcholines (PC, $n = 28$), Lysophosphatidyl-choline (LPC, $n = 11$) and Sphingomyelins (SM, $n = 13$) from RYGB ($n = 8$) and Sham ($n = 6$) lymph samples. Lipids were extracted by a methyl-tert-butyl ether (MTBE) protocol as previously described [22]. Data acquisition was performed on an LTQ Orbitrap Velos Pro instrument (Thermo Scientific) coupled to a Dionex Ultimate 3000 UHPLC (Thermo Scientific) according to previously published protocols [23,24]. Briefly, chromatographic separation was performed on a Waters (Waters, Milford, MA, USA) BEH C8 column (100 × 1 mm, 1.7 μm), and the mass spectrometer was operated in Data Dependent Acquisition (DDA) mode. Full scan profile spectra were acquired in the Orbitrap mass analyzer at a resolution setting of 100,000. For MS/MS experiments, the 10 most abundant ions of the full scan spectrum were sequentially fragmented. Data analysis was performed by Lipid Data Analyzer, a custom software described in Hartler et al. [25,26].

2.7. Enterocyte isolation and real time quantitative polymerase chain reaction (RT-qPCR) analysis

Rats were food deprived overnight and sacrificed by anesthetized decapitation. A piece of distal jejunum was dissected from 5 cm oral to the cecum, inverted, and washed in phosphate-buffered saline (PBS, Gibco). The mucosa was carefully scraped off with a glass slide, immediately frozen with liquid nitrogen, and kept at −80 °C until further processing. RNA was extracted using Trizol reagent (Life Technologies #15596018) following the manufacturer's protocol and treated with DNAse (Qiagen #79254). cDNA was synthesized using the High-Capacity cDNA Reverse Transcription Kit (Applied Biosystems #4368813). RT-qPCR reactions were run in triplicates using FAST SYBR green and the Viia7 Real Time PCR system (Applied Biosystems). The $2^{-\Delta\Delta CT}$ method was used for analysis with β-actin as the reference gene. Primer sequences are listed in Supplemental Table 1.

2.8. Oil red O (ORO) staining

Rats were food deprived overnight and sacrificed by anesthetized decapitation. The most distal 2 cm of the jejunum were taken for the histological analysis. After rinsing with PBS, the intestinal samples were fixed in 4% paraformaldehyde, cryoprotected in 30% sucrose, and embedded in OCT embedding matrix (81-0771-00; Biosystems AG). ORO staining was performed on 6 μm sections following the manufacturer's protocol (ab150678, Abcam) with hematoxylin counterstaining (517-28-2; Sigma–Aldrich) and Aqua Perm Mounting Medium (Thermo Scientific #484980). Image analysis of the ORO staining was done with ImageJ, version 1.50b (National Institutes of Health, USA) as described by Mehlem et al. [27]. Area of red pixels was determined and represented as percentage of the whole villus area.

2.9. Primary enterocyte fatty acid oxidation (FAO) assay

Primary enterocytes of fasted animals or of animals 30 min after a HFD TM, were isolated from the distal jejunum, 5–20 cm proximal to the cecum as described earlier [28,29]. After 20 min in a cell recovery solution (#354253, Corning) the cells were transferred to supplemented DMEM (Gibco #A1443001) as described before with the only difference that 200,000 living cells were plated [30]. For the FAO assay, the cells were incubated for 6 h with 5 mM glucose, 500 μM L-carnitine, 50 μM fatty acid free BSA, 100 μM palmitic acid and 2 μCi/mL of (^{3}H-9,10)-palmitic acid 37 °C, 5% CO_2 incubator). Subsequently, supernatants were transferred into a crystal vial, added 3 M perchloric acid to stop residual metabolic activity, and enclosed in the presence of water-soaked filter paper as described in Veys et al. [31]. Vials were incubated for 48 h at 37 °C. The disintegrations per minute were recorded using the 2000CA liquid scintillation analyzer (Tri-Carb) using Ultima Gold scintillation fluid (Perkin Elmer #6013329).

2.10. Fatty acid uptake (FAU) assay

Enterocytes (of fasted animals or of animals 30 min after a HFD TM) were isolated as described above. Bodipy-C12 (Molecular Probes #D3823) was pre-incubated with fatty acid–free bovine serum albumin (BSA) (2:1 M ratio) in PBS as described earlier [32]. Before resuspension with matrigel and plating, the cell pellet was incubated with Bodipy-FA conjugated with BSA (Bodipy-FA/BSA) for 5 min at 37 °C. Cells were washed twice and plated (200,000 living cells/well) in 0.5% BSA in PBS and 0.4% trypan blue (MP Biomedicals #1691049). Intracellular fluorescence was measured (bottom-read) with a microplate reader (excitation 503 nm, emission 548 nm, Spark 10M).

2.11. Data analysis

2.11.1. Multivariate exploratory analysis of lipidomics data

z-Standardized concentrations of 183 lipid classes 21 days after surgery were analyzed by principal component analysis using the FactoMineR package [33] and by hierarchical clustering using Ward's criterion. The optimal number of clusters was determined with the gap statistics methods [34].

2.11.2. Identification of lipids regulated by RYGB

We used two methods to identify lipid classes whose concentration in intestinal lymph differed between RYGB and Sham rats 21 days after surgery: the volcano plot (base-2 logarithm of fold change (FC) above 1 or below −1 and base-10 logarithm of the *P*-value below −2), and Partial Least Squares Discriminant Analysis (PLS-DA) using MetaboAnalyst (Variable Importance in Projection (VIP) scores > 1.0). Lipids identified by both the volcano plot and the VIP scores were used for further analysis (Supplementary Figure 2).

2.11.3. Data presentation

Data are presented as means ± SEM, unless boxplots are drawn. All analyses and graphs were generated using GraphPad Prism (versions 6.05 and 7.02), or R studio (version 1.1.453).

2.11.4. Statistical analysis

Statistical tests used and results are given in each figure legend. When applicable, data normality was verified using the Shapiro–Wilk (when $n \geq 7$) and the Kolmogorov–Smirnov (when $n \leq 6$) tests, and homoscedasticity was checked by visualizing the distribution of residuals. Non-parametric tests were used otherwise. *p*-Values < 0.05 were considered significant.

3. RESULTS

3.1. RYGB reduces post-prandial TG levels in the plasma and the intestinal lymph

As a result of HFD exposure, rats randomized to Sham or RYGB surgery were pre-surgically heavier and less glucose tolerant than their LFD

littermates (Supplementary Figure 1). From Day 10 after surgery and onwards, RYGB rats weighed less than Sham rats (Figure 1A). On Day 14, RYGB rats' glucose tolerance was improved compared to Sham rats (Figure 1B) such that their glucose AUC appeared similar to the one of LFD rats (Data not shown). Our rat RYGB model therefore exhibited the hallmarks of RYGB-induced rapid weight loss and improved glucose tolerance. Systemic plasma TG levels were lower in RYGB than Sham rats 30 min after the 2.5 g TM. This gap narrowed at 4 h fasting and disappeared after 16 h fasting, when both groups had low plasma TG levels (Figure 1C). Also, 30 min after the TM, plasma cholesterol levels were lower in RYGB rats than in Sham rats (Figure 1D).

We then tested whether RYGB reduces TM-induced TG levels in the intestinal lymph, a direct readout of enterocyte lipid secretion (Figure 2A). After an identical 2.5 g TM, RYGB rats also had lower overall TG concentrations than Sham rats in the intestinal lymph (Figure 2B). These results indicate that RYGB reduces postprandial intestinal TG secretion compared to Sham.

3.2. RYGB reduces selectively TG and DG levels in intestinal lymph

We then examined whether RYGB reduces intestinal TG secretion specifically or whether it also affects other lipid classes. We therefore applied mass spectrometry lipidomics to the intestinal lymph of RYGB and Sham rats taken after a 2.5 g TM (0–21 days after surgery). Lipidomics analysis from samples prior to RYGB/Sham surgery did not reveal any differences between the two groups (data not shown). We first tested whether the overall lipid composition of intestinal lymph differed 21 d after RYGB and Sham surgery based on z-standardized concentrations of 183 detected lipid classes. In PCA analysis, 95% confidence ellipses around RYGB and Sham rats did not overlap in the two first dimensions (representing 48.7% and 19.8% of the overall inertia — Figure 3A). Similarly, hierarchical cluster analysis separated RYGB and Sham rats in two non-overlapping groups (Figure 3B). The clustered heatmap of *z*-standardized lipid concentrations (Figure 3C) revealed that most, but not all, of the tested lipid classes were decreased 21 d after RYGB compared to Sham. Together, these results indicate that RYGB substantially modifies the overall intestinal lymph lipid profile. When analyzing the relative change of total concentration by lipid classes, it became apparent that TG and DG were downregulated more than other lipid classes (Figure 3D). Beyond the total concentration of lipid classes, we also tested whether single TG and DG were over-represented among all downregulated single lipids. We used the volcano plot (Figure 3E) and the VIP score of the PLS-DA (Supplementary Figure 2A) to identify lipids modulated by RYGB. Both methods led to the identification of 65 lipid classes (Supplementary Figure 2B/C) whose levels were changed 21 days after RYGB (61 down, 4 up). The pool of downregulated lipids differed in composition from the pool of detected lipids, with a clear overrepresentation of single TG and DG species (Figure 3F). The extent of downregulation of the TG and DG species was similar between 10 and 21 days after surgery (Supplementary Figure 2D), suggesting that the reported effects are not acute artefacts of the surgery.

Together, the lipidomics analysis of intestinal lymph revealed an overall downregulation of intestinal lipid secretion after RYGB, but with major differences among lipid classes. TG and DG species downregulated most, indicating a selective process.

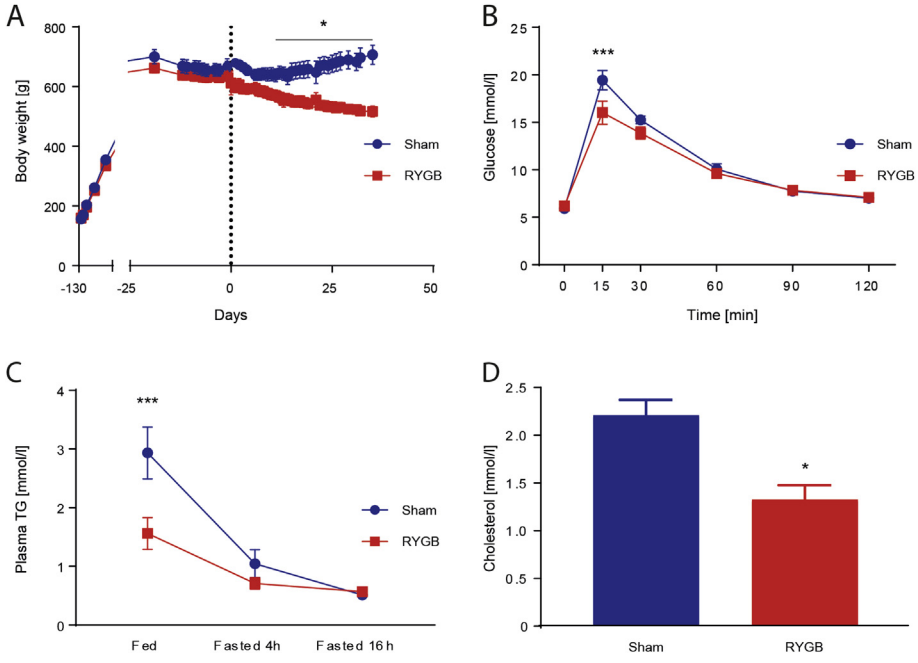

Figure 1: RYGB decreased BW and improved insulin sensitivity. (A) Body weight [$n = 6/8$; Two-way ANOVA, Interaction (surgical group × time), $P < 0.0001$, significant difference from day 10 on (Sidak's multiple comparisons test $P < 0.05$)]. Similar average pre-surgical BW (RYGB: 636 ± 18, Sham: 631 ± 28, $P > 0.999$). On postoperative day 30 (RYGB/Sham surgery is indicated by dashed line), the BW difference was 165 g (RYGB: 525 ± 16, Sham: 690 ± 31, $P < 0.001$). Data represent means ± SEM. (B) IPGTT in Week 2 after surgery [$n = 8/6$; Two-way ANOVA, Interaction (surgical group × time) $P < 0.05$, Sidak's multiple comparisons test: P 15 min < 0.005]. (C) Plasma TG levels measured in a fed state (30 min after a TM), after 4 h of fasting and after 16 h of fasting [$n = 6/8$; Two-way ANOVA, Interaction (surgical group × time) $P < 0.05$, Sidak's multiple comparisons test: P fed $= 0.0005$; P fasted 4 h $= 0.67$; P fasted 6 h $= 0.9971$]. (D) Plasma cholesterol concentrations 30 min after the TM [$n = 5/6$; Student t-test $P < 0.05$].

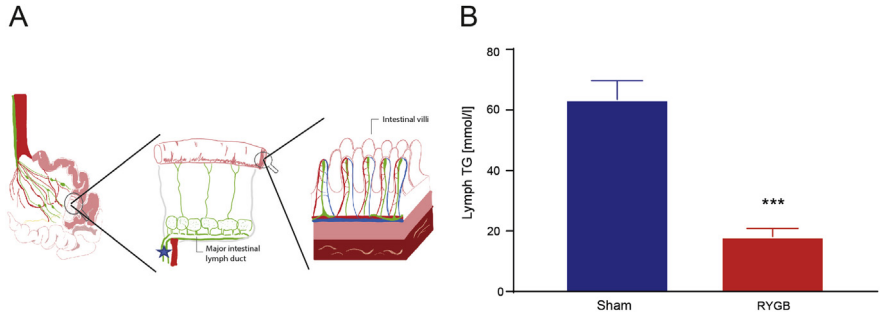

Figure 2: RYGB leads to reduced postprandial TG concentrations in intestinal lymph. (A) Schematic depiction of the cannula placement in the intestinal lymph duct. Red: arterial blood vessels, blue: venous blood vessels, green: lymph vessels, star: cannula placement (B) TG concentrations in intestinal lymph, measured with the same method as in the blood, replicating the results seen in plasma [$n = 5/6$; Student t-test $P < 0.001$].

3.3. RYGB-induced decreases in lymph TG and DG levels depend on chain-length and saturation

Based on the observation that three long-chain TG species with unsaturated fatty acids (TG60:6, TG60:7, TG62:7) were upregulated (and not downregulated) the intestinal lymph 21 days after RYGB (Supplementary Figure 2C), we examined whether RYGB modulates TG and DG species levels based on the chain-length and saturation. We found significant positive correlations between the cumulative chain-

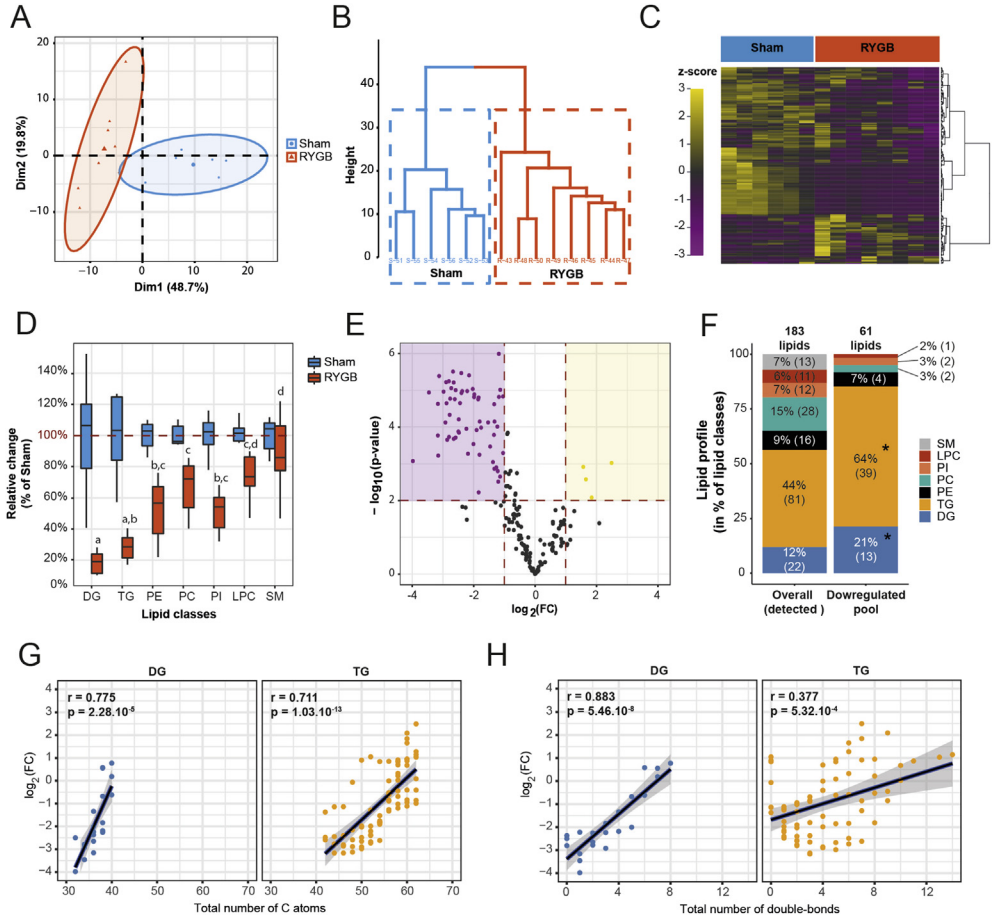

Figure 3: RYGB modulates the lymph lipidome and specifically affects short-chain, saturated di- and triglycerides. (A) Individual plot with 95% confidence ellipses in the 2 first dimensions of a principal component analysis (total inertia = 68.5%). (B) Hierarchical clustering with Ward's criterion and (C) Heatmap of z-standardized molar concentrations of 183 detected lymph lipids 21 days after surgery [$n = 6/8$]. (D) Relative reduction in total lipid concentration by subtype by RYGB 21 days after surgery [$n = 6/8$; ANOVA; subtype effect $P < 0.0001$; letters indicate significant differences between subtypes with Tukey multiple comparisons]. (E) Volcano plot of all 183 lipids detected in the lymph [$n = 6/8$; FC between RYGB and Sham 21 days after surgery; P-values correspond to Student t-tests of single lipid concentrations between RYGB and Sham 21 days after surgery]. (F) Lipid subtype profile of all detected lipids (183) and all lipids downregulated in RYGB compared to Sham (61) [$n = 6/8$; difference in the distribution of lipids among subtypes was tested with Fisher's exact test for count data with Monte-Carlo simulated P-value 10,000 replicates; $P < 0.01$]. (G) Correlation between total number of carbon atoms or (H) total number of double-bounds and FC (log 2) of single lipid concentrations between RYGB and Sham rats 21 days after surgery [$n = 6/8$; r and P indicate the Pearson's product moment correlation values and P-values between FC and total number of carbon atoms or double bonds; Linear regression lines are shown with their 95% confidence intervals].

length and FC after RYGB for TG and DG (Figure 3G). Similarly, significant positive correlations were apparent between the total number of double bonds and FC after RYGB for TG and DG (Figure 3H). No other lipid classes consistently showed similar correlations between FC and cumulative chain length or cumulative number of double bonds (Supplementary Figure 3A, B). Together, these findings indicate that upon RYGB the composition of DG and TG secreted by the intestine is shifted towards long-chain, unsaturated lipid classes.

3.4. RYGB reprograms enterocyte lipid handling

Considering the specific reduction of intestinal TG and DG secretion after RYGB, we tested whether RYGB affects enterocytes' fatty acid absorption, reesterification, storage in lipid droplets, and oxidation using transcriptional and functional assays. RYGB reduced the expression of lipid uptake genes (*Fatp4*, *Fabp2*, *Cd36*) in enterocytes of 16 h fasted rats (Figure 4A). We then assessed FAU functionally using the fluorescent fatty acid Bodipy-C12 in primary enterocytes of Sham and RYGB rats: consistently with the transcriptional data, FAU was reduced in 16 h fasted RYGB rats compared to Sham rats (Figure 4B). Thirty minutes after a HFD TM, however, FAU was increased in RYGB rats compared to Sham (Figure 4B).

Second, consistent with the RYGB-induced changes in the intestinal lipidome, we found that RYGB reduced the expression of genes known to affect chylomicron composition and size (*Apob*, *Apoa4*) in 16 h fasted rats (Figure 4A). Intriguingly, these transcriptional changes were accompanied by an increased expression of the main genes involved in TG re-esterification (*Dgat1*, *Mgat2*).

Third, because enterocyte lipid droplets can act as buffers to prevent postprandial hypertriglyceridemia [14,35], we quantified lipid droplets in jejunal sections stained with ORO. We found a trend towards a greater amount of ORO staining expressed as red pixel percentage, i.e., more (=bigger areas of) lipid droplets in RYGB rat enterocytes compared to Sham rat enterocytes (Figure 4D). Villus length and villus area were also increased in RYGB rat enterocytes (data not shown). Together this suggests an increased presence of lipid droplets and neutral lipids in the common limb of RYGB rats. A fourth pathway that could modify the composition of lipids secreted by the intestine is the oxidation of fatty acids within enterocytes; therefore, we functionally

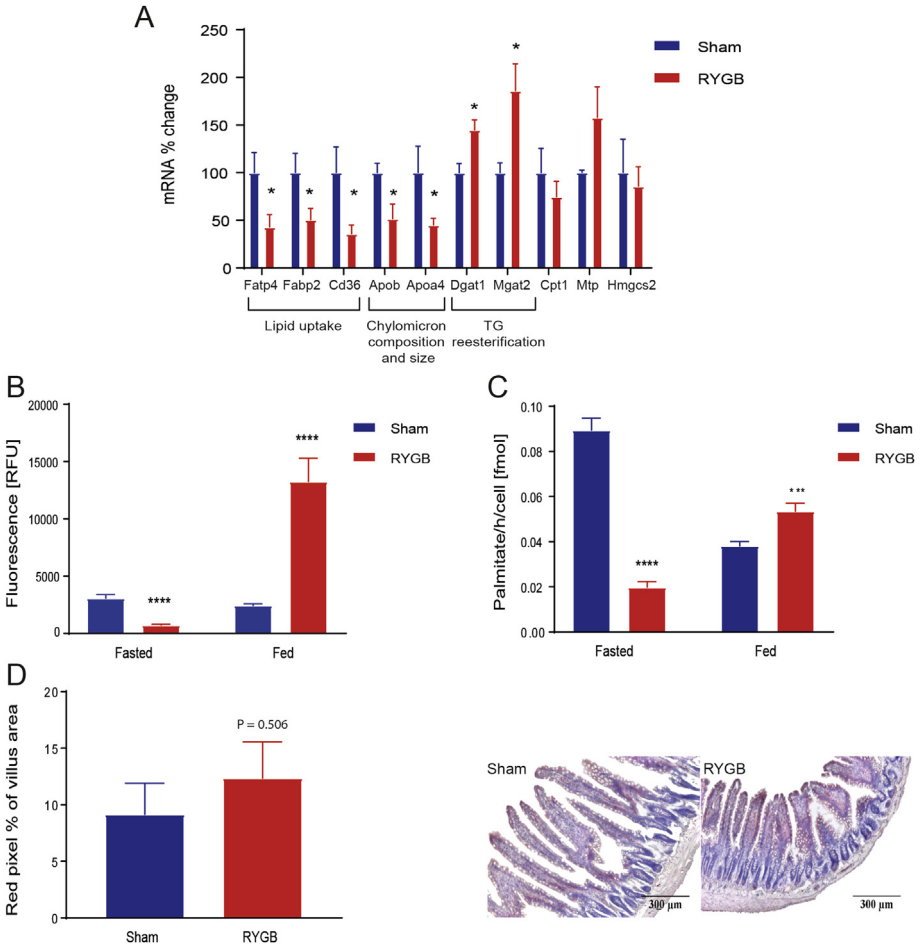

Figure 4: RYGB affects the expression of key genes implicated in lipid transport and absorption, in lipid droplet storage and FAO. (A) Enterocyte gene expression levels of genes related to lipid absorption, resynthesis, secretion, or storage in the fasted state. [$n = 6/8$; Student *t*-tests: *Fatp4*: Fatty acid transport protein 4, $P < 0.05$; *Fabp2*: fatty acid binding protein 2, $P < 0.05$; *Cd36*: fatty acid translocase, $P < 0.05$; *Acsl5*: acyl-CoA synthetase long-chain family member 5, $P < 0.05$; *Cpt1*: Carnitine palmitoyltransferase 1, $P = 0.4026$; *Mgat1*: Alpha-1,6-mannosyl-glycoprotein 2-beta-N-acetylglucosaminyltransferase, $P < 0.05$; *Dgat1*: Diglyceride acyltransferase 1, $P < 0.05$; *Mtp*: Microsomal triglyceride transfer protein, $P = 0.1578$; *Apob*: Apolipoprotein B, $P < 0.05$; *Apoa4*: Apolipoprotein A-IV, $P < 0.05$]. Data are presented as mean values ± SEM. (B–C) FAU and FAO in isolated enterocytes in a fasted and fed (30 min after a TM) state [n (biological) = 3; n (technical) = 6/8; Student *t*-tests: FAU and FAO: P fasted < 0.0005; P fed < 0.005]. (D) ORO stained intestinal cross-sections of a representative Sham animal (A) and a representative RYGB animal (B) [$n = 3/4$, ×50 magnification] after an overnight fast. Higher villus area for RYGB animals, $P < 0.0001$. (E) Red pixel % [$n = 3/4$, P = 0.5060].

investigated enterocyte FAO using labeled palmitic acid. We found a reduced palmitic acid oxidation in primary enterocytes of 16 h fasted RYGB rats compared to Sham rats but an enhanced FAO in the enterocytes of RYGB rats after the TM compared to Sham rats (Figure 4C). Thus, RYGB modulates fatty acid uptake in the enterocytes dependent on the feeding status. In addition, RYGB shifts the intracellular balance in enterocyte lipid handling: TG release pathways are repressed whereas postprandial FAO and storage in lipid droplets are favored (or at least maintained) compared to Sham.

4. DISCUSSION

RYGB rapidly reduces plasma TG levels in humans through yet unidentified mechanisms [1]. Here we show that in a rat model of RYGB, reduced postprandial TG concentrations, well documented in the plasma, are also evident in the intestinal lymph, indicating that postprandial enterocyte TG secretion is reduced in RYGB compared to Sham rats. Using lipidomics analysis of postprandial intestinal lymph samples, we demonstrate that RYGB affected the intestinal lymph lipid profile in general and specifically reduced DG and TG. In addition, RYGB differentially affected individual DG and TG species, augmenting those with long-chain, unsaturated fatty acids. Finally, these changes were associated with a reprogramming of enterocyte lipid handling, consistent with a reduction in TG secretion and changes in FAO and lipid storage in the enterocytes. Together, our data show that RYGB substantially modifies enterocyte TG absorption, handling, and secretion in rats, and strongly suggest that intestinal adaptations contribute to the improvements in plasma TG profile seen after RYGB. As the observed differences were already present ten days after the surgery, our data indicate that the intestine plays a major role in the rapid drop in plasma DG and TG concentrations documented after RYGB, reversing the high levels of those lipids in overweight humans [36]. A unique strength of our study was the use of intestinal lymph sampling, which provides the most direct readout of enterocyte lipid secretion [19]. This allowed for the specific observation of RYGB-induced changes in intestinal lipid handling and for uncoupling these changes from peripheral TG metabolism that is markedly influenced by the concomitant improvements in insulin sensitivity.

At first glance, the extent to which RYGB reduced lipid concentrations in intestinal lymph compared to Sham surgery after an identical TM raises the question of fat malabsorption. In humans, increases in fecal fat content after RYGB have been repeatedly documented [1,37,38] and are believed to originate from a reduced time for ingested lipids to emulsify with bile acids. As we did not measure fecal fat content concomitant with controlled dietary fat intake, we cannot exclude that fat malabsorption influenced the postprandial intestinal lymph lipidome. Nevertheless, another study showed that the extent of fecal fat excretion is limited in rat models of RYGB, and is not considered as the main cause of changes in plasma lipid levels [39]. In addition, the specific pattern of the intestinal lymph TG and DG after RYGB (chain-length and saturation-specific changes), as well as the increase in concentrations of certain lipids, also argue against a general decrease in lipid absorption. Finally, our finding that RYGB broadly reshapes enterocyte lipid handling pathways and lipid accumulation in a fasted state is not consistent with a major role of fat malabsorption. On the energy intake side, we cannot fully exclude that some of the differences in the lymph lipid profile might be due to the chronic differences in the nutrient load between Sham and RYGB rats.

The exact mechanisms explaining the specific reduction of postprandial enterocyte TG secretion after RYGB require further investigation. First, we found a reduced *Cd36* expression in the enterocyte of fasted RYGB rats compared to Sham. Interestingly, *Cd36*-null mice show reduced TG synthesis in the endoplasmic reticulum and reduced secretion as chylomicrons [40]. It is therefore plausible that the decrease in enterocyte *Cd36* expression in RYGB plays a causal role in the specific downregulation of TG in the intestinal lymph. The decreased *Fabp2* expression in the enterocytes of RYGB rats compared to Sham also contribute because *Fabp2*-null mice also show significant decreases in FA incorporation into TG relative to phospholipids [41]. Finally, the finding that TG and DG with longer-chain, unsaturated FA were "preserved" after RYGB may be related to the observed upregulation in *Dgat1*. Indeed, *Dgat1* affinity is particularly high for longer, unsaturated fatty acids for reesterification [42], which may have favored the reesterification of these fatty acids over shorter chain, saturated fatty acids.

Beyond the known association between reduced TG levels and CVD, RYGB-induced changes in the intestinal lipidome may also be relevant for the improvements in glucose homeostasis. Specifically, the finding that DG and TG with long-chain, unsaturated fatty acids are preserved in the intestinal lymph of RYGB rats may be beneficial because the presence of these lipids is associated with a decreased risk of developing diabetes [43], whereas saturated circulating lipids are known markers of insulin resistance [44]. In a 12-year follow-up of the Framingham cohort study, the association between carbon number, double bond content and the risk of developing diabetes was strongest for TG and persisted after adjustments for other known diabetes risk factors, including total TG levels and HDL cholesterol. Interestingly, four of the six TG most associated with an increased risk of diabetes described in the Framingham cohort were reduced by RYGB in our study (TG44:1; TG46:1; TG48:1; TG52:1) [43]. The association between plasma lipids with higher carbon number and double bond content and insulin sensitivity is not fully understood, but is believed to be mediated by the fatty acid composition of cell membranes [45], such that saturated fatty acyl in phospholipids alter membrane fluidity, insulin receptor binding or affinity and decrease the effectiveness of glucose transport. In addition, the downregulation of intestinal DG secretion after RYGB may also positively affect glucose homeostasis because DG recruit and activate nPKCθ, which then leads to inhibitory phosphorylation of insulin receptor substrate 1 and ultimately to a decreased glucose uptake into the cell [18].

One discrepancy between our findings and plasma lipidomics analyses performed in humans after RYGB is that we did not see the reduction in SM observed in humans [46,47]. Unlike other lipid classes, however, plasma SM levels are significantly lower in rats than humans [48], which may make it difficult to detect a decrease. Using a DDA approach, we did not acquire the single fatty acid structure of the lipids but the whole lipid composition of each single lipid. This limited us in the ability to compare our findings to identified potential biomarkers. On the other hand, the animal model avoids many confounding factors such as dietary restrictions, voluntary and involuntary changes in dietary intake, or changes in food preference that occur in human patients. Furthermore, it is not possible (yet) to measure intestinal lymph composition in humans. In particular, for lipidomics analysis, it was important to keep the RYGB and Sham rats on the exact same lipid composition/diet in order to investigate the enterocyte (such as desaturation and elongation) effects.

The improvements in plasma lipids in humans after RYGB are commonly ascribed to changes in dietary intake and improvement in insulin sensitivity. Our data indicate that, in addition to these effects, changes in intestinal lipid handling and secretion are likely to contribute to RYGB-induced improvements in plasma lipids and the related reduction in cardiovascular mortality and insulin resistance

[49]. Our data therefore support the current view that the beneficial metabolic effects of RYGB may be mediated by intestinal adaptation [50] and specifically through adaptations of the enterocytes themselves. Reports of reduced postprandial lipid levels in other surgical models such as the Vertical Sleeve Gastrectomy extend this idea that the intestine is a major player in causing the beneficial effects of weight-loss surgeries [51]. Perhaps most striking is the finding that, although given the same HFD TM as Sham rats, RYGB rats showed an intestinal lymph lipidome that would be expected after a meal with lower fat content, and displayed a lipidome whose profile of TG with long-chain unsaturated fatty acids is commonly associated with cardiovascular health and insulin sensitivity. Understanding how RYGB exerts these effects may lead to novel approaches targeting enterocyte metabolism and lipid handling pathways in the quest of bariatric surgery mimetics.

ACKNOWLEDGMENTS

We thank Marcella Martins Terra and Nino Jejelava for the support with lymph sampling and Karin Kaufman for designing and preparing the schematic of the lymph duct cannulation. Financial support was provided by Boehringer Ingelheim Fonds and ETH Zurich.

CONFLICTS OF INTEREST

None.

APPENDIX A. SUPPLEMENTARY DATA

Supplementary data to this article can be found online at https://doi.org/10.1016/j.molmet.2019.03.002.

REFERENCES

[1] Carswell, K.A., Belgaumkar, A.P., Amiel, S.A., Patel, A.G., 2016. A systematic review and meta-analysis of the effect of gastric bypass surgery on plasma lipid levels. Obesity Surgery 26(4):843–855. https://doi.org/10.1007/s11695-015-1829-x.

[2] Sjöström, L., Peltonen, M., Jacobson, P., Sjöström, C.D., Karason, K., Wedel, H., et al., 2012. Bariatric surgery and long-term cardiovascular events. JAMA 307(1):56. https://doi.org/10.1001/jama.2011.1914.

[3] Adams, T.D., Gress, R.E., Smith, S.C., Halverson, R.C., Simper, S.C., Rosamond, W.D., et al., 2007. Long-term mortality after gastric bypass surgery. New England Journal of Medicine 357(8):753–761. https://doi.org/10.1056/NEJMoa066603.

[4] Yusuf, S., Hawken, S., Ounpuu, S., Dans, T., Avezum, A., Lanas, F., et al., 2004. Effect of potentially modifiable risk factors associated with myocardial infarction in 52 countries (the INTERHEART study): case control study. The Lancet 364(9438):937–952. https://doi.org/10.1016/S0140-6736(04)17018-9.

[5] Heffron, S.P., Parikh, A., Volodarskiy, A., Ren-Fielding, C., Schwartzbard, A., Nicholson, J., et al., 2016. Changes in lipid profile of obese patients following contemporary bariatric surgery: a meta-analysis. The American Journal of Medicine 129(9):952–959. https://doi.org/10.1016/j.amjmed.2016.02.004.

[6] Adams, T.D., Davidson, L.E., Litwin, S.E., Hunt, S.C., 2012. Gastrointestinal surgery: cardiovascular risk reduction and improved long-term survival in patients with obesity and diabetes. Current Atherosclerosis Reports 14(6):606–615. https://doi.org/10.1007/s11883-012-0286-4.

[7] Osto, E., Doytcheva, P., Corteville, C., Bueter, M., Dörig, C., Stivala, S., et al., 2015. Rapid and body weight-independent improvement of endothelial and high-density lipoprotein function after Roux-en-Y gastric bypass role of glucagon-like peptide-1. Circulation 131(10):871–881. https://doi.org/10.1161/circulationaha.114.011791.

[8] Wickremesekera, K., Miller, G., DeSilva Naotunne, T., Knowles, G., Stubbs, R.S., 2005. Loss of insulin resistance after Roux-en-Y gastric bypass surgery: a time course study. Obesity Surgery 15(4):474–481. https://doi.org/10.1381/0960892053723402.

[9] Jørgensen, N.B., Dirksen, C., Bojsen-Møller, K.N., Kristiansen, V.B., Wulff, B.S., Rainteau, D., et al., 2015. Improvements in glucose metabolism early after gastric bypass surgery are not explained by increases in total bile acids and fibroblast growth factor 19 concentrations. Journal of Clinical Endocrinology & Metabolism 100(3):E396–E406. https://doi.org/10.1210/jc.2014-1658.

[10] Spinelli, V., Lalloyer, F., Baud, G., Osto, E., Kouach, M., Daoudi, M., et al., 2016. Influence of Roux-en-Y gastric bypass on plasma bile acid profiles: a comparative study between rats, pigs and humans. International Journal of Obesity 40(8):1260–1267. https://doi.org/10.1038/ijo.2016.46.

[11] Zechner, J.F., Mirshahi, U.L., Satapati, S., Berglund, E.D., Rossi, J., Scott, M.M., et al., 2013. Weight-independent effects of roux-en-Y gastric bypass on glucose homeostasis via melanocortin-4 receptors in mice and humans. Gastroenterology 144(3):580–590. https://doi.org/10.1053/j.gastro.2012.11.022 e7.

[12] Xiao, C., Stahel, P., Carreiro, A.L., Buhman, K.K., Lewis, G.F., 2018. Recent advances in triacylglycerol mobilization by the gut. Trends in Endocrinology and Metabolism 29(3):151–163. https://doi.org/10.1016/j.tem.2017.12.001.

[13] Hussain, M.M., 2014. Intestinal lipid absorption and lipoprotein formation. Current Opinion in Lipidology 25(3):200–206. https://doi.org/10.1097/mol.0000000000000084.

[14] D'Aquila, T., Hung, Y.-H., Carreiro, A., Buhman, K.K., 2016. Recent discoveries on absorption of dietary fat: presence, synthesis, and metabolism of cytoplasmic lipid droplets within enterocytes. Biochimica et Biophysica Acta (BBA) – Molecular and Cell Biology of Lipids 1861(8):730–747. https://doi.org/10.1016/j.bbalip.2016.04.012.

[15] le Roux, C.W., Borg, C., Wallis, K., Vincent, R.P., Bueter, M., Goodlad, R., et al., 2010. Gut hypertrophy after gastric bypass is associated with increased glucagon-like peptide 2 and intestinal crypt cell proliferation. Annals of Surgery 252(1):50–56. https://doi.org/10.1097/SLA.0b013e3181d3d21f.

[16] Hansen, C.F., Bueter, M., Theis, N., Lutz, T., Paulsen, S., Dalbøge, L.S., et al., 2013. Hypertrophy dependent doubling of L-cells in Roux-en-Y gastric bypass operated rats. PLoS One 8(6). https://doi.org/10.1371/journal.pone.0065696.

[17] Saeidi, N., Meoli, L., Nestoridi, E., Gupta, N.K., Kvas, S., Kucharczyk, J., et al., 2013. Reprogramming of intestinal glucose metabolism and glycemic control in rats after gastric bypass. Science 341(6144):406–410. https://doi.org/10.1126/science.1235103.

[18] Erion, D.M., Shulman, G.I., 2010. Diacylglycerol-mediated insulin resistance. Nature Medicine 16(4):400–402. https://doi.org/10.1038/nm0410-400.

[19] Arnold, M., Dai, Y., Tso, P., Langhans, W., 2012. Meal-contingent intestinal lymph sampling from awake, unrestrained rats. The Australian Journal of Pharmacy: Regulatory, Integrative and Comparative Physiology 302(12):R1365–R1371. https://doi.org/10.1152/ajpregu.00497.2011.

[20] Bueter, M., Abegg, K., Seyfried, F., Lutz, T.A., le Roux, C.W., 2012. Roux-en-Y gastric bypass operation in rats. Journal of Visualized Experiments(64):6–11. https://doi.org/10.3791/3940.

[21] Jejelava, N., Kaufman, S., Krieger, J.-P., Terra, M.M., Langhans, W., Arnold, M., 2018. Intestinal lymph as a readout of meal-induced GLP-1 release in an unrestrained rat model. American Journal of Physiology – Regulatory, Integrative and Comparative Physiology 314(5):R724–R733. https://doi.org/10.1152/ajpregu.00120.2017.

[22] Matyash, V., Liebisch, G., Kurzchalia, T.V., Shevchenko, A., Schwudke, D., 2008. Lipid extraction by methyl-*tert*-butyl ether for high-throughput lipidomics. Journal of Lipid Research 49(5):1137–1146. https://doi.org/10.1194/jlr.D700041-JLR200.

[23] Triebl, A., Trötzmüller, M., Hartler, J., Stojakovic, T., Köfeler, H.C., 2017. Lipidomics by ultrahigh performance liquid chromatography-high resolution mass spectrometry and its application to complex biological samples. Journal of Chromatography B: Analytical Technologies in the Biomedical and Life Sciences 1053:72–80. https://doi.org/10.1016/j.jchromb.2017.03.027.

[24] Fauland, A., Köfeler, H., Trötzmüller, M., Knopf, A., Hartler, J., Eberl, A., et al., 2011. A comprehensive method for lipid profiling by liquid chromatography-ion cyclotron resonance mass spectrometry. Journal of Lipid Research 52(12): 2314–2322. https://doi.org/10.1194/jlr.D016550.

[25] Hartler, J., Trötzmüller, M., Chitraju, C., Spener, F., Köfeler, H.C., Thallinger, G.G., 2011. Lipid data analyzer: unattended identification and quantitation of lipids in LC–MS data. Bioinformatics 27(4):572–577. https://doi.org/10.1093/bioinformatics/btq699.

[26] Hartler, J., Triebl, A., Ziegl, A., Trötzmüller, M., Rechberger, G.N., Zeleznik, O.A., et al., 2017. Deciphering lipid structures based on platform-independent decision rules. Nature Methods 14(12):1171–1174. https://doi.org/10.1038/nmeth.4470.

[27] Mehlem, A., Hagberg, C.E., Muhl, L., Eriksson, U., Falkevall, A., 2013. Imaging of neutral lipids by oil red O for analyzing the metabolic status in health and disease. Nature Protocols 8(6):1149–1154. https://doi.org/10.1038/nprot.2013.055.

[28] Nik, A.M., Carlsson, P., 2013. Separation of intact intestinal epithelium from mesenchyme. BioTechniques 55(1):42–44. https://doi.org/10.2144/000114055.

[29] Ramachandran, D., Clara, R., Fedele, S., Hu, J., Lackzo, E., Huang, J.Y., et al., 2017. Intestinal SIRT3 overexpression in mice improves whole body glucose homeostasis independent of body weight. Molecular Metabolism 6(10):1264–1273. https://doi.org/10.1016/j.molmet.2017.07.009.

[30] Ramachandran, D., Clara, R., Fedele, S., Michel, L., Burkard, J., Kaufman, S., et al., 2018. Enhancing enterocyte fatty acid oxidation in mice affects glycemic control depending on dietary fat. Scientific Reports 8(1):1–13. https://doi.org/10.1038/s41598-018-29139-6.

[31] Veys, K., Alvarado-Diaz, A., De Bock, K., 2019. Measuring glycolytic and mitochondrial fluxes in endothelial cells using radioactive tracers. Metabolic Signaling: Methods and Protocols 12:121–136.

[32] Jang, C., Oh, S.F., Wada, S., Rowe, G.C., Liu, L., Chan, M.C., et al., 2016. A branched-chain amino acid metabolite drives vascular fatty acid transport and causes insulin resistance. Nature Medicine 22(4):421–426. https://doi.org/10.1038/nm.4057.

[33] Lê, S., Josse, J., Husson, F., 2008. FactoMineR: an {R} package for multivariate analysis. Journal of Statistical Software 25(1):1–18. https://doi.org/10.1016/j.envint.2008.06.007.

[34] Kassambara, A., Mundt, F., 2016. Factoextra: extract and visualize the results of multivariate data analyses.

[35] Beilstein, F., Carrière, V., Leturque, A., Demignot, S., 2016. Characteristics and functions of lipid droplets and associated proteins in enterocytes. Experimental Cell Research 340(2):172–179. https://doi.org/10.1016/j.yexcr.2015.09.018.

[36] Graessler, J., Schwudke, D., Schwarz, P.E.H., Herzog, R., Schevchenko, A., Bornstein, S.R., 2009. Top-down lipidomics reveals ether lipid deficiency in blood plasma of hypertensive patients. PLoS One 4(7). https://doi.org/10.1371/journal.pone.0006261.

[37] Odstrcil, E.A., Martinez, J.G., Ana, C.A.S., Xue, B., Schneider, R.E., Steffer, K.J., et al., 2010. The contribution of malabsorption to the reduction in net energy absorption after long-limb Roux-en-Y gastric bypass. American Journal of Clinical Nutrition 1–3:704–713. https://doi.org/10.3945/ajcn.2010.29870.704.

[38] Kumar, R., Lieske, J.C., Collazo-Clavell, M.L., Sarr, M.G., Olson, E.R., Vrtiska, T.J., et al., 2011. Fat malabsorption and increased intestinal oxalate absorption are common after roux-en-Y gastric bypass surgery. Surgery 149(5):654–661. https://doi.org/10.1016/j.surg.2010.11.015.

[39] Stylopoulos, N., Hoppin, A.G., Kaplan, L.M., 2009. Roux-en-Y gastric bypass enhances energy expenditure and extends lifespan in diet-induced obese rats. Obesity 17(10):1839–1847. https://doi.org/10.1038/oby.2009.207.

[40] Drover, V.A., Ajmal, M., Nassir, F., Davidson, N.O., Nauli, A.M., Sahoo, D., et al., 2005. CD36 deficiency impairs intestinal lipid secretion and clearance of chylomicrons from the blood. Journal of Clinical Investigation 115(5):1290–1297. https://doi.org/10.1172/JCI21514.

[41] Gajda, A.M., Zhou, Y.X., Agellon, L.B., Fried, S.K., Kodukula, S., Fortson, W., et al., 2013. Direct comparison of mice null for liver or intestinal fatty acid-binding proteins reveals highly divergent phenotypic responses to high fat feeding. Journal of Biological Chemistry 288(42):30330–30344. https://doi.org/10.1074/jbc.M113.501676.

[42] Cses, S., Stone, S.J., Zhou, P., Yen, E., Tow, B., Lardizabal, K.D., et al., 2001. Cloning of DGAT2, a second mammalian diacylglycerol acyltransferase, and related family members. Journal of Biological Chemistry 276(42):38870–38876. https://doi.org/10.1074/jbc.M106219200.

[43] Rhee, E.P., Cheng, S., Larson, M.G., Walford, G.A., Lewis, G.D., McCabe, E., et al., 2011. Lipid profiling identifies a triacylglycerol signature of insulin resistance and improves diabetes prediction in humans. Journal of Clinical Investigation 121(4):1402–1411. https://doi.org/10.1172/JCI44442.

[44] Kotronen, A., Velagapudi, V.R., Yetukuri, L., Westerbacka, J., Bergholm, R., Ekroos, K., et al., 2009. Serum saturated fatty acids containing triacylglycerols are better markers of insulin resistance than total serum triacylglycerol concentrations. Diabetologia 52(4):684–690. https://doi.org/10.1007/s00125-009-1282-2.

[45] N.M. Weijers, R., 2012. Lipid composition of cell membranes and its relevance in type 2 diabetes mellitus. Current Diabetes Reviews 8(5):390–400. https://doi.org/10.2174/157339912802083531.

[46] Kayser, B.D., Lhomme, M., Dao, M.C., Ichou, F., Bouillot, J.L., Prifti, E., et al., 2017. Serum lipidomics reveals early differential effects of gastric bypass compared with banding on phospholipids and sphingolipids independent of differences in weight loss. International Journal of Obesity 41(6):917–925. https://doi.org/10.1038/ijo.2017.63.

[47] Arora, T., Velagapudi, V., Pournaras, D.J., Welbourn, R., Le Roux, C.W., Orešič, M., et al., 2015. Roux-en-Y gastric bypass surgery induces early plasma metabolomic and lipidomic alterations in humans associated with diabetes remission. PLoS One 10(5):e0126401. https://doi.org/10.1371/journal.pone.0126401.

[48] Ishikawa, M., Saito, K., Urata, M., Kumagai, Y., Maekawa, K., Saito, Y., 2015. Comparison of circulating lipid profiles between fasting humans and three animal species used in preclinical studies: mice, rats and rabbits. Lipids in Health and Disease 14(1):1–6. https://doi.org/10.1186/s12944-015-0104-4.

[49] Christou, N.V., Sampalis, J.S., Liberman, M., Look, D., Auger, S., McLean, A.P.H., et al., 2004. Surgery decreases long-term mortality, morbidity, and health care use in morbidly obese patients. Annals of Surgery 240(3):416–424. https://doi.org/10.1097/01.sla.0000137343.63376.19.

[50] Sinclair, P., Brennan, D.J., Le Roux, C.W., 2018. Gut adaptation after metabolic surgery and its influences on the brain, liver and cancer. Nature Reviews Gastroenterology & Hepatology. https://doi.org/10.1038/s41575-018-0057-y.

[51] Stefater, M.A., Sandoval, D.A., Chambers, A.P., Wilsonpérez, H.E., Hofmann, S.M., Jandacek, R., et al., 2011. Sleeve gastrectomy in rats improves postprandial lipid clearance by reducing intestinal triglyceride secretion. Gastroenterology 141(3):939–949. https://doi.org/10.1053/j.gastro.2011.05.008 e4.

